THE JOURNAL OF PHYSICAL CHEMISTRY C

Article

pubs.acs.org/JPCC

Dielectric Study of Hydration Water in Silica Nanoparticles

Silvina Cerveny,*[,‡] Gustavo A. Schwartz,[‡,∥] Jon Otegui,[‡] Juan Colmenero,[‡,§,∥] Juliane Loichen,[†] and Stephan Westermann[†]

[†]Global Materials Science, Goodyear Innovation Center Luxembourg, Avenue Gordon Smith, L-7750 Colmar-Berg, Luxembourg

[‡]Centro de Fisica de Materiales (CFM, CSIC/UPV) - Materials Physics Center (MPC), Paseo Manuel de Lardizabal 5, 20018 San Sebastián, Spain

[§]Facultad de Química, Departamento de Física de Materiales, UPV/EHU, 20018 San Sebastián, Spain

[∥]Donostia International Physics Center, 20018 San Sebastián, Spain

Supporting Information

ABSTRACT: The effect of water content on silica nanoparticles was examined by thermogravimetry analysis (TGA), broadband dielectric spectroscopy (from 10^{-2} to 10^{7} Hz), and differential scanning calorimetry for a wide temperature range (110−250 K). Silica nanoparticles were dried and rehydrated at different water levels to determine the critical factors affecting the dielectric response. The dynamics of both hydration water and hydrated silanol groups were addressed. Whereas hydration water dynamics depend on the water content, the dynamics corresponding to hydrated silanol groups are almost water independent once the maximum hydroxylation level is reached. In addition, we determined that during hydration water molecules prefer to form clusters instead of filling a complete layer around the particles. Finally, we observed that contrary to other water containing systems, the corresponding relaxation times of water molecules do not show any crossover (from high-T super-Arrhenius to low-T Arrhenius behavior).

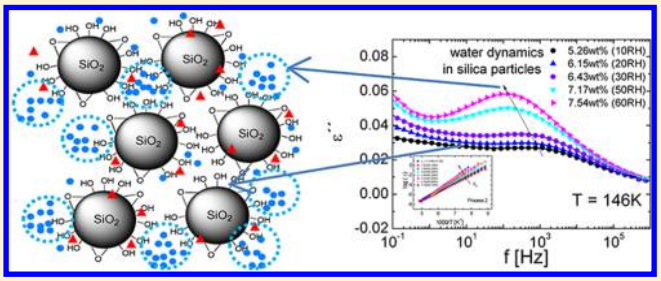

INTRODUCTION

The introduction of nanoparticles with an extremely large specific surface into polymeric materials improves several characteristics of the compound such as electrical, optical, or mechanical properties. In particular, amorphous silica plays a significant role in many different disciplines of chemistry, and it has become widely used as an integral component of several industrial products. Silica nanoparticles can easily be prepared; they possess a high chemical stability and environmentally friendly nature,[1] and therefore they are used in many products (such us plastics, adhesives, paints and coatings, insulation materials, elastomers, or concrete). The optical, chemical, and mechanical properties of the final products strongly depend on the chemistry of the particles' surfaces; in particular on the concentration and distribution of both hydroxyl groups and water molecules on its surface.

Silica (silicon dioxide, SiO_2) is the major constituent of rock-forming minerals in magmatic and metamorphic rocks.[2] Precipitated silica particles are the synthetic, white, amorphous form of silicon dioxide, and they consist of silicon and oxygen atoms arranged in a tetrahedral structure of a three-dimensional lattice. The surface of precipitated silicas is covered by silanol groups (−Si−OH) which can be divided into three kinds: isolated or free silanol (O≡Si−OH), the geminal silanol or silanediol group [two −OH hydroxyl groups on the same silicon atom, O═Si═$(OH)_2$], and vicinal silanol (hydrogen bonded silanol groups) as illustrated in Figure 1. The number of free, vicinal or geminal silanol groups on the silica surface depends on the calcination temperature. In addition, hydrophobic (and nonpolar) siloxane groups (Si−O−Si) are also present. Free silanols can develop hydrogen bonds, and therefore they promote interparticle hydrogen bonding. In addition, the terminal hydroxyl groups promote the adsorption of water and other polar molecules, and the amount of water adsorption is directly related to the number of surface hydroxyl groups.[3]

Precipitated silica particles are used in numerous applications but the oldest and most important is the reinforcement of elastomeric products such as tire compounds, cables, or shoe soles.[1] The addition of 20−100 parts by weight of precipitated silica to 100 parts by weight of synthetic rubbers improves the tensile strength, hardness, and abrasion of the vulcanized material.[2] When silica particles are used as reinforcement, water molecules as well as hydroxyl groups remain on its surface, and they play an important role in compounding which is not yet well understood.[4] For this reason, it is crucial to understand at first how water interacts with silica particles in order to control its properties and optimize the surface of the particles for different applications.

Received: August 7, 2012
Revised: October 26, 2012
Published: October 28, 2012

dx.doi.org/10.1021/jp307826s | J. Phys. Chem. C 2012, 116, 24340−24349

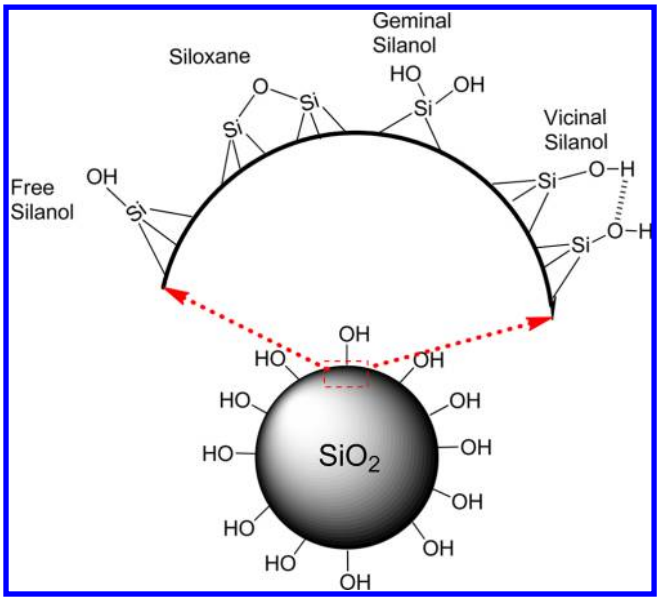

Figure 1. Clasification of silanol groups on the surface of silica particles.

The molecular properties of silica particles and other siliceous materials such as mesoporous molecular sieves (MCM-41) or zeolites were mainly studied in the literature by using a combination of different techniques: thermogravimetry, vibrational spectroscopy (i.e., Fourier transform infrared spectroscopy (IR), Raman, diffuse or total reflectance IR, and photoacoustic IR), and solid-state NMR spectroscopy[5−11]). These studies were focused on the surface structure, surface chemistry, and water adsorption on silica particles. Dielectric studies of water confined in MCM-41 and similar materials have also been published.[12−16] These studies were mainly focused on the dynamics of water in deeply supercooled states, itself, more than in the matrix. Finally, in addition to these experimental studies, Zuravlev,[17,18] based on results of different experimental techniques, develops a model for the dehydration, dehydroxylation, and rehydroxylation states of the surface of amorphous silica. Although dielectric studies could provide some insight of the water dynamics on the silica surface, studies regarding the dynamical response of silica particles are missing in the literature.

In this article, we report a systematic study by means of broadband dielectric spectroscopy (BDS) of the dynamics of both the hydration water molecules and hydroxyl groups of the silica particles surface considering a broad water concentration range. We will focus on the effects of both drying temperature and hydration level on the dielectric response. In addition, calorimetric and thermogravimetric experiments were also performed to complete the characterization of the materials. We will show that two main relaxation processes are observed at low temperatures (110−250 K), and they are interpreted as fluctuations of clusters of water molecules and hydrated silanol groups on the surface of silica particles, respectively.

EXPERIMENTAL SECTION

Materials and Silica Hydration. Precipitated silica particles (Z1165 MP-Rhodia) with a specific surface, $S_{specific}$ = 165.8 m^2/g (mean diameter of the primary particles is ∼25 nm) and pore volume = 1.74 cm^3/g were used in this work. First, silica particles were extensively dried at 393 K in a vacuum oven for 3 days. At this temperature most of the water was evaporated, although some water molecules could remain extremely trapped on the silica structure (inner water). In addition, silanol groups on the silica surface also remain. After this drying, silica was immediately weighed and transferred to a hydration chamber where both the relative humidity (RH) and the temperature can be controlled. Silica particles were hydrated by exposing them at different relative humidities (from 10 RH to 80 RH) at a temperature of 295 K. The samples were maintained at a constant relative humidity for 4 days in order to achieve the equilibrium for each hydration level. Once the silica particles were hydrated to the desired

Table 1. Samples Used in This Work[a]

Silica Particles Dried at Different Temperatures								
				process 2		process 3		
sample identification	drying temperature (K)	$c_{w,total}$ (wt %)	$c_{w,outer}$ (wt %)	E_a (eV)	log(τ_0)	E_a (eV)	log(τ_0)	Θ
S-923K	923	0.02	–	–	–	–	–	–
S-393K	393	2.76	0	–	–	0.59	−21.40	–
S-373K	373	4.88	2.12	0.34	−15.73	0.62	−21.55	0.38
Silica Particles Exposed at Different Humidity Levels								
				process 2		process 3		
sample identification	relative humidity (RH)	$c_{w,total}$ (wt %)	$c_{w,outer}$ (wt %)	E_a (eV)	log(τ_0)	E_a (eV)	log(τ_0)	Θ
S-10RH	10	5.26	2.50	0.34	−15.56	0.57	−19.93	0.45
S-20RH	20	6.15	3.39	0.37	−16.61	0.58	−20.14	0.60
S-30RH	30	6.43	3.67	0.39	−16.99	0.58	−20.32	0.66
S-40RH	40	6.71	3.95	0.43	−18.43	0.57	−19.64	0.71
S-50RH	50	7.17	4.41	0.46	−18.92	0.59	−20.35	0.79
S-60RH	60	7.54	4.78	0.49	−20.02	0.74	−24.88	0.85
S-70RH	70	8.55	5.79	0.48	−19.52	–	–	1.03
S-80RH	80	11.23	8.47	0.52	−20.66	–	–	1.51

[a]The total water content ($c_{w,total}$) was calculated as the loss weight at 433 K from thermogravimetry analysis (TGA) measurements. The total water content is calculated with respect to dry silica. $c_{w,outer}$ is defined as the water in the external surface, and it was calculated as $c_{w,outer} = c_{w,total} - 2.76$. E_a is the activation energy, and log(τ_0) is the pre-exponential factor corresponding to processes 2 and 3 in Figure 6. Θ is the number of water layers at the surface of the silica particles estimated as $c_{w,outer}/5.88$.

dx.doi.org/10.1021/jp307826s | J. Phys. Chem. C 2012, 116, 24340−24349

level, samples were weighed and immediately measured. Additionally, one sample was dried under vacuum for 3 days at 373 K, and one more was dried for 1 day at 923 K under a nitrogen atmosphere. Table 1 shows both the relative humidity and the water content reached at each humidity level calculated from thermogravimetric measurements.

Alternatively, following the work of Spanoudaki et al.[13] and Meier et al.,[19] it is possible to estimate the water content necessary to obtain a monolayer of water on the silica surface by assuming a hexagonal arrangement of the water molecules on the surface. Assuming a lattice constant d = 3.2 Å, which corresponds to the size of a water molecule, the water content necessary to form a monolayer ($c_{w,mono}$) around a particle can be estimated as

$$h_{mono} = S_{specific} \frac{2}{\sqrt{3}\, d^2} \frac{M_{H_2O}}{N_A} \quad (1)$$

where M_{H_2O} is the molar mass of water, and N_A is Avogadro's number. For our silica particles, the water content corresponding to a monolayer is $c_{w,mono}$ = 5.6 wt %, in agreement with Meier et al.[19] Table 1 shows the number of water layers found with each water content calculated as $\Theta = c_{w,outer}/c_{w,mono}$.

Thermal Characterization. Standard calorimetric measurements were performed by means of a differential scanning calorimeter (DSC) Q2000 (TA Instrument) using cooling and heating rates of 10 K/min. Hermetic aluminum pans were used for all of the samples. The sample weight was about 10 mg. Thermogravimetric analyses were done using a TGA-Q500 (TA Instruments). All the measurements were conducted under a high-purity nitrogen flow over a temperature range of 303−1273 K with a ramp rate of 5 K/min.

Broadband Dielectric Spectroscopy. Broadband dielectric spectroscopy (BDS) is a technique based on the interaction of an external field with the electric dipole moment of the molecules of the sample.[20] With this technique, it is possible to study the molecular dynamics over a broad frequency (from 10^{-6} to 10^{+11} Hz) and temperature (100−350 K) range. To perform a dielectric measurement, the sample is placed between two metallic electrodes which form a capacitor. For the parallel-plate configuration, the capacitance is expressed as $C = \varepsilon d/A$, where ε is the dielectric permittivity of the sample, A is the sample surface area, and d its thickness. The material properties are characterized by the complex dielectric permittivity, ε^*, which is defined as $\varepsilon^*(\omega) = C^*(\omega)/C_0 = \varepsilon'(\omega) - i\varepsilon''(\omega)$, where C_0 is the capacitance of the free space and $\omega = 2\pi f$.

A broadband dielectric spectrometer, Novocontrol Alpha analyzer, was used to measure the complex dielectric function, $\varepsilon^*(\omega) = \varepsilon'(\omega) - i\varepsilon''(\omega)$, in the frequency range from 10^{-2} to 10^{7} Hz. The samples were prepared by placing the silica particles between two parallel gold-plated electrodes (30 mm in diameter) with the thickness of about 0.5 mm. Isothermal frequency scans were performed every three degrees over the temperature range 110−200 K, and every five degrees from 255 to 300 K. Sample temperature was controlled by a nitrogen gas flow with stability better than ±0.1 K.

RESULTS

Thermal characterization. Figure 2 shows the results of the thermogravimetric analysis for some dried and hydrated silica particles. Three typical steps on the thermograms are observed (seen as peaks in the derivative plot in the inset of Figure 2). The first rapid initial drop of the mass (from room temperature up to ~473 K) corresponds with the loss of both adsorbed water on the silica surface and structurally bound water within the silica skeleton.[17] Above 473 K, vicinal and geminal silanol groups on silica particles are condensed to siloxanes, and this is seen as a weight drop in a broad temperature range from 473 to 873 K. In this broad temperature range, free silanols are still stable. Finally, the last drop (from 873 to 1273 K) corresponds with the release of free siloxanes and other thermal decompositions.[17,18] The total moisture content (c_w, expressed as grams of water per grams of dry particles) for hydrated- and vacuum-dried silica particles was calculated as the loss of mass at 433 K divided by the sample weight at the same temperature. The results are shown in Table 1.

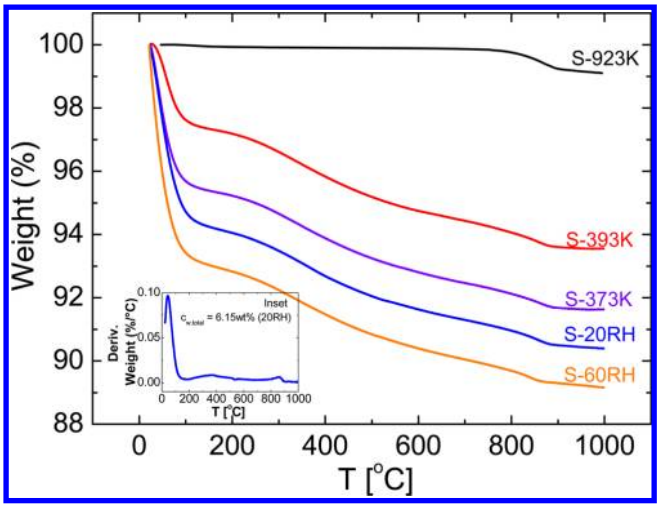

Figure 2. Thermogravimetric measurements (TGA) of the loss mass up to 1273 K for different silica particles as indicated in the figure. The inset shows the weight derivative plot for silica particles hydrated at 20 RH.

Thermal behavior of silica particles was characterized by DSC and the results are shown in Figure 3. No calorimetric features (on cooling or heating) were observed for samples with water content lower than 8 wt % (~65 RH), and therefore water remains amorphous in the whole temperature range analyzed (see dashed line). In addition, for the sample with $c_{w,total}$ = 8.55 wt %, a small exothermic peak on cooling was observed in the calorimetric response, indicating water crystallization (see solid line). The inset in Figure 3 reports the calorimetric response of the sample S-80RH at a cooling and heating rate of 1 K/min. At this slow cooling rate, two clear peaks observed (at 232 K and 223 K, respectively) are indicative of two water populations in the samples at high hydration levels. The behavior of this crystalline sample will not be further discussed in this paper.

Dielectric Response of Silica Particles. Figure 4 (panels a and b) shows the isothermal dielectric loss spectra for silica particles dried at 373 K and 393 K, respectively. The dielectric loss spectra $\varepsilon''(\omega)$ for the least dried sample (S-373K) exhibit three relaxation processes labeled 1, 2, and 3 from the fastest one to the slowest one (see Figure 5, panels a and b). As it will be discussed in the next section, process 2 is due to the relaxation of water molecules in the outer shell, whereas process 3 is mainly due to the reorientation of hydrated vicinal/geminal silanol groups. Process 1 appears only at very low temperatures (between 100 and 125 K), and it is required to appropriately fit the dielectric response at high frequencies/low temperatures.

dx.doi.org/10.1021/jp307826s | J. Phys. Chem. C 2012, 116, 24340−24349

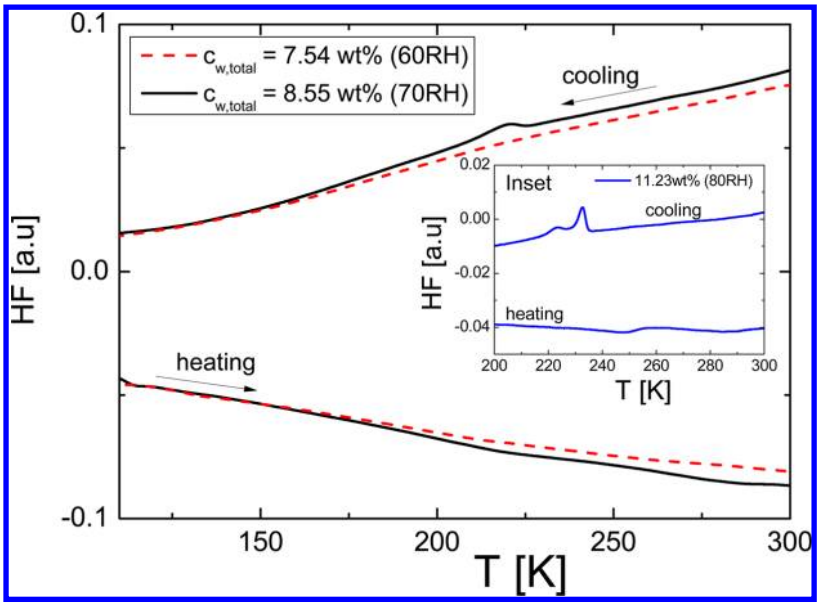

Figure 3. Heat flow measured by DSC during cooling and heating at a rate of 10 K/min for silica particles with two water contents. No calorimetric features are observed in silica hydrated up to a $c_{w,total}$ of 7.54 wt %. However, crystallization and melting peaks due to water crystallization are observed in the sample with $c_{w,total}$ = 8.55 wt %. The inset shows the calorimetric response, for a narrower temperature range, at a rate of 1 K/min for hydrated silica at $c_{w,total}$ = 11.23 wt %.

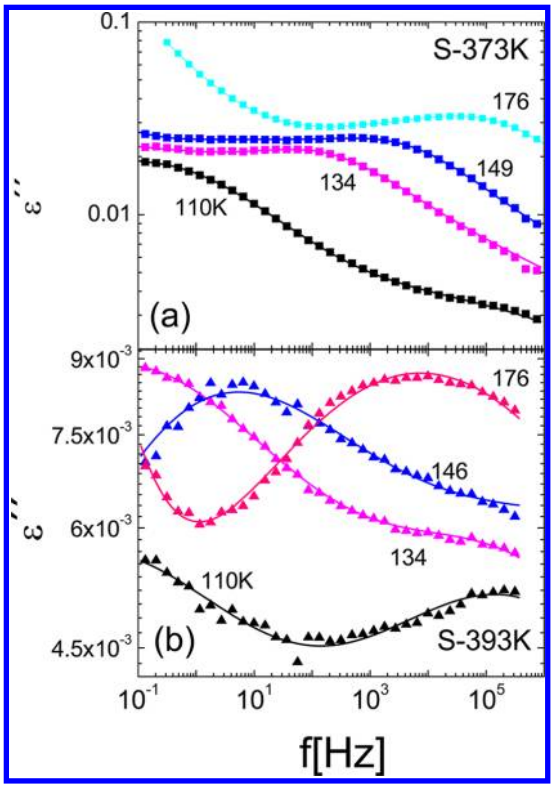

Figure 4. Dielectric loss spectra of (a) S-373K and (b) S-393K measured at different temperatures (110, 134, 149, and 176 K). The solid line through the data points represents the fits to the experimental data.

By increasing the drying temperature at 393 K (sample S-393K), the dielectric spectra of silica particles reveal only two relaxation processes (1 and 3 in correspondence with that in sample S-373K, see Figure 5b). In addition, for the sample S-923K, no processes were detected in the dielectric response in the broad frequency/temperature range analyzed.

Figure 6a shows the isothermal dielectric loss spectra at T = 146 K for dried samples together with one of the hydrated samples. By increasing the drying temperature from 373 to 923 K, the dielectric signal progressively becomes broader and weaker until it almost disappears at the highest drying temperature. Note that the behavior of the least hydrated sample (S-10RH, $c_{w,total}$ = 5.26 wt %) is similar to that of the sample S-373K as they have a similar water content.

Figure 6b shows the dielectric response for hydrated samples at different water concentrations at T = 146 K. Two processes, a well-resolved peak at high frequencies (process 2) and a shoulder at low frequencies (process 3) can be observed. By increasing the water content, two effects on the dielectric signal can be observed: the total dielectric signal increases and the main relaxation peak (process 2) moves to lower frequencies. Due to this, process 2 masks process 3 at a high water content. In order to appropriately describe the data of the hydrated samples (as previously discussed for dried samples), an extra process at low temperatures/high frequency (process 1) is necessary to describe the dielectric data. Therefore, the dielectric response of hydrated samples can also be described with three dielectric relaxation processes, similar to those used for sample S-373K.

Fitting Procedure and Shape Parameters. Each of the relaxation processes above-mentioned have been analyzed in terms of the Cole−Cole (CC) function since all the processes are symmetric. The Cole−Cole function is defined by[21]

$$\varepsilon^*(\omega) = \varepsilon_\infty + \frac{\Delta\varepsilon}{[1 + (i\omega\tau)^\alpha]} \quad (2)$$

where α is the shape parameter that determines the symmetric broadening of the relaxation peak ($0 < \alpha \leq 1$); $\Delta\varepsilon = \varepsilon_s - \varepsilon_\infty$, is the relaxation strength, and ε_∞ and ε_s are the unrelaxed and relaxed values of the dielectric constant. τ is a characteristic relaxation time, and ω is the angular frequency.

At low temperatures (lower than 140 K), two processes are visible in our frequency window (see Figure 5a). In this case,

dx.doi.org/10.1021/jp307826s | J. Phys. Chem. C 2012, 116, 24340−24349

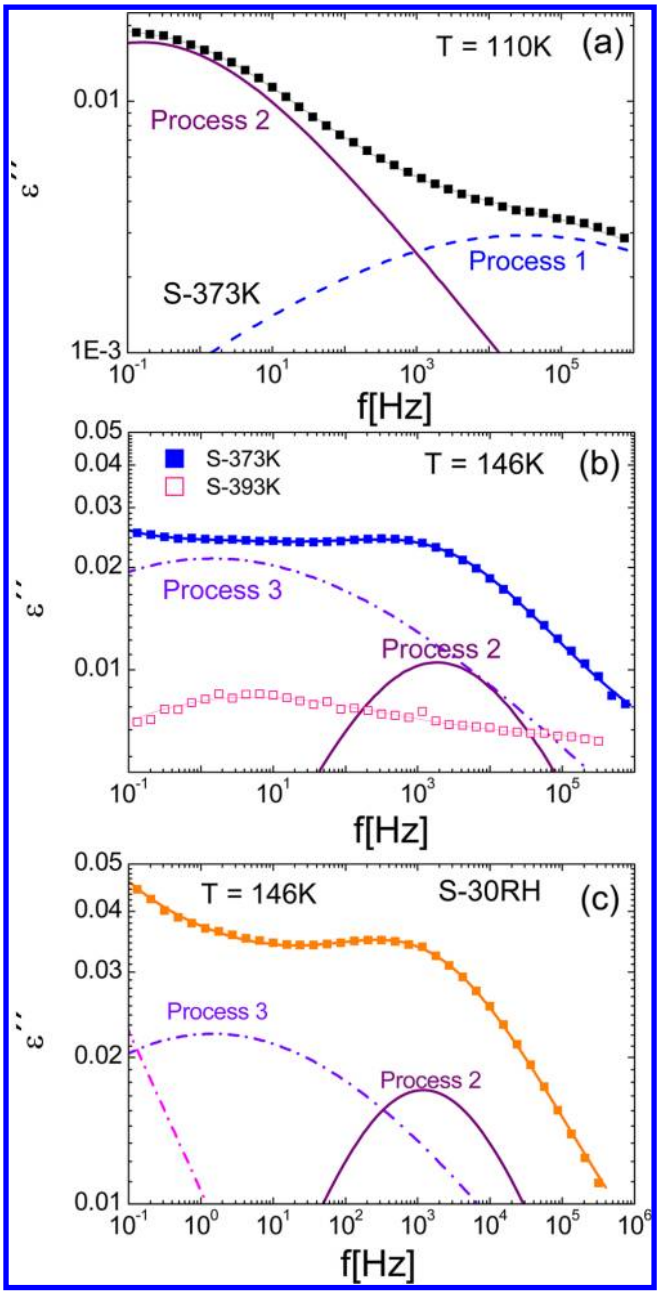

Figure 5. (a) Dielectric loss spectrum at a fixed temperature (110 K) of S-373K. Processes 1 (dashed line) and 2 (solid line) denote the two dielectric processes observed at this temperature. (b) Dielectric loss spectra at T = 146 K of S-373K and S-393K. At this temperature, processes 2 (solid line) and 3 (dashed dotted line) are observed. (c) Dielectric loss spectra at T = 146 K of S-30RH. At this temperature, processes 2 (solid line) and 3 (dashed dotted line) are observed. For all of the figures, the solid line through the data points represents the fits to the experimental data.

two CC functions were used to describe the whole spectrum at each temperature. At higher temperatures, between 140 K and 220 K, two processes are also observed in our frequency window (processes 2 and 3), and therefore two CC functions were used to describe the spectrum at each temperature. In addition, at low frequencies, conductivity effects become dominant (from approximately 160 K), and a power law term was added to the sum of CC functions. All the parameters were left free during the fitting procedure. Solid lines through the data points in both Figures (5 and 6) show the best fit to the experimental data.

The relaxation strength obtained from the fitting procedure corresponding to process 2 ($\Delta\varepsilon_2$) is temperature independent in the T-range here analyzed (see Figure S1 of the Supporting Information) but depends on the amount of water. In Figure 7, average values of $\Delta\varepsilon_2$ were plotted as a function of c_w. The dielectric strength increases almost linearly up to a water content of 3.5 wt %. At a higher water content, $\Delta\varepsilon_2$ deviates from this behavior increasing much faster. Finally, when water crystallization starts, the dielectric strength decreases because less water molecules are involved in this relaxation process because some of them become part of the ice network (see the arrow in Figure 7). With regards to α_2 (see Figure S2 of the Supporting Information), it slightly increases with temperature and becomes systematically smaller by increasing the water content, indicating a more heterogeneous environment. Regarding process 3, the relaxation strength ($\Delta\varepsilon_3$) is also temperature independent, and the average value increases from 0.07 to 0.19 from samples S-393K to S-373K. Besides that, $\Delta\varepsilon_3$ is more or less constant for the rest of the water content, and this indicates that the intensity of this relaxation is not related to the level of hydration in the samples.

Relaxation Map. Figure 8a shows the relaxation map for sample S-373K where the three above-mentioned processes (1, 2, and 3) can be observed. In addition, Figure 8b shows how process 2 becomes slower with an increasing water content. Contrarily, the relaxation time corresponding to process 3 (Figure 8c) slightly changes with water content. This behavior reflects the fact that it is possible to distinguish between different types of dipoles relaxing on the sample. The relaxation time for all of these processes follows an Arrhenius behavior [$\tau = \tau_0 \exp(E_a/kT)$] in the whole temperature range here analyzed. The activation energies, E_a, and $\log(\tau_0)$, were calculated, and both values are shown in Table 1 for the processes 2 and 3. For process 1, the activation energy is E_a = 0.11 eV and $\log(\tau_0) = -10.70$ s.

DISCUSSION

As mentioned in the introduction, the surface of silica particles is covered by polar silanol groups (isolated, vicinal, or geminal) as well as apolar siloxanes (−Si−O−Si−). These silanols have a strong dipole moment comparable with that of water molecules (1.85D). As dielectric spectroscopy is sensitive to fluctuations of dipole moments, it is not surprising to observe two different dynamics related to the two dipolar species in hydrated silica (water molecules and silanol groups). In addition, modeling of physical and chemical properties of the amorphous silica−water interface has been reported in the literature.[22] Hassanali and Singer[22] pointed out the evidence for the affinity of water molecules for silanol groups. Also the existence of "hydrophobic regions" (regions with high density of siloxanes) on the silica surface was observed. The existence of these regions leads to water clustering. In this work, we study silica particles with an increasing water content. This methodology allows for the distinguishing of two different dielectric relaxations: the slower one (process 3), which is almost independent of the hydration level, and the other one (process 2), faster and clearly dependent on the hydration level. With all these ideas in mind, we are going to discuss the dielectric behavior of both dried and hydrated silica particles.

Dielectric Response of Dried Silica Particles. We start the discussion with the most dried sample (S-923K). The silica

dx.doi.org/10.1021/jp307826s | J. Phys. Chem. C 2012, 116, 24340−24349

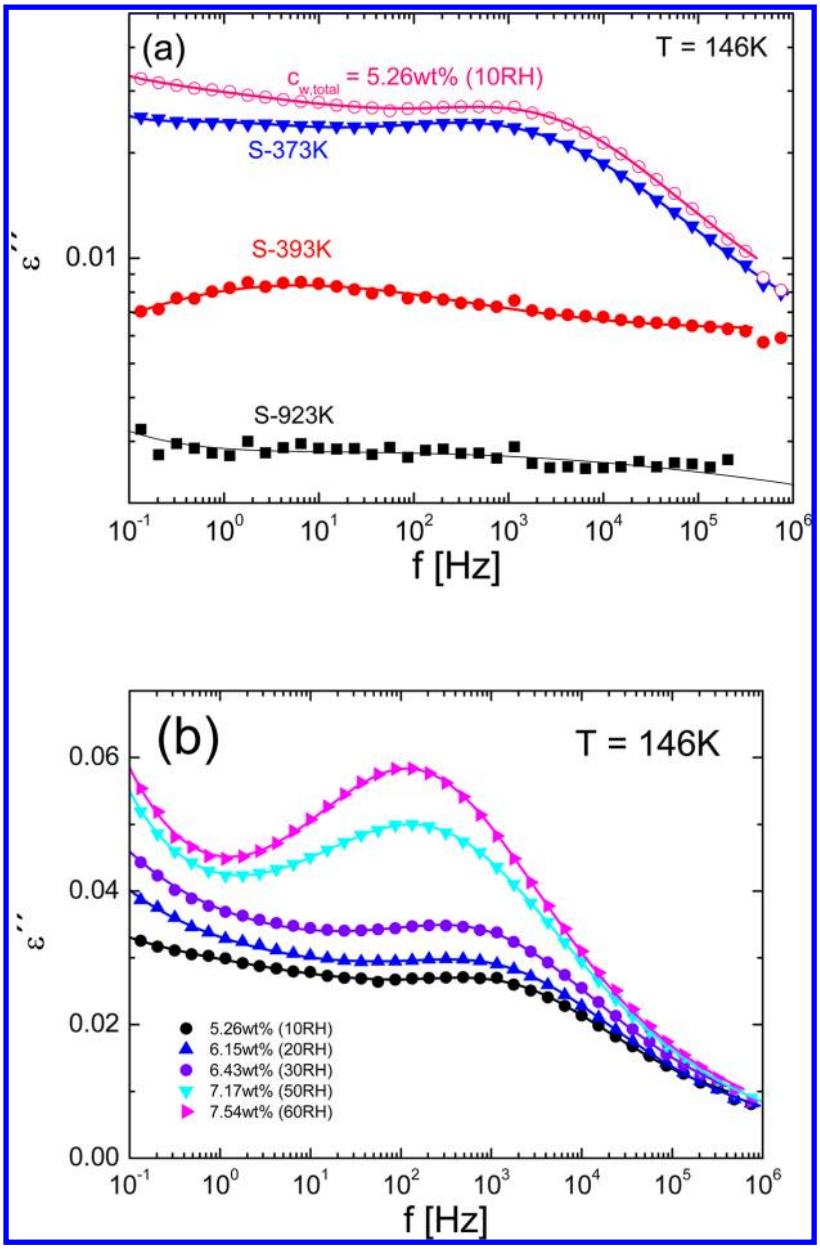

Figure 6. (a) Comparison of the dielectric loss spectra at a fixed temperature (146 K) of silica particles dried under vacuum. (b) Dielectric loss spectra at a fixed temperature (146 K) of hydrated silica particles. The solid line through the data points represents the fits to the experimental data.

particles lost most of the silanol groups (only a few free silanol groups remain), and its surface is mainly covered by siloxane groups. We have confirmed the absence of vicinal or geminal silanol groups by means of thermogravimetric measurements, since there is no weight loss in the temperature region between 473 and 873 K (see Figure 2). Taking into account that no dielectric processes were observed for this sample (where only siloxanes and a small quantity of free silanol groups remain on the surface), we can conclude that both siloxane groups and free silanols do not substantially contribute to the dielectric response.

For the sample dried at 393 K (S-393K), most of the water molecules on the surface are removed. However, a water content of 2.76 wt % remains (as detected by TGA). These water molecules are mostly located on the inner surface of the particles. We define this fraction of water as the internal water content or "inner water content" in the silica particles ($c_{w,inner}$ = 2.76 wt %) in the sense that these water molecules are hardly removed by standard drying. As shown in Figure 5b and 6a, the dielectric response of sample S-393K shows a single relaxation peak (process 3). We also note that by drying at 393 K, the particle surface remains in a state of maximum hydroxylation,[17] and therefore the reorientation of silanols on the surface (which have a large dipolar moment, comparable with that of water molecules) can be attributed as the origin of this relaxation. This assignment includes only the hydroxyl groups in the vicinal or geminal silanol groups, since previously we have shown (for sample S-923K) that free silanols do not appreciably contribute to the dielectric response. Note, at first view, that we cannot discard the "inner water" as the origin of this relaxation. However, the temperature dependence of the relaxation times do not show the typical crossover from super-Arrhenius to Arrhenius behavior by decreasing the temperature, typical of confined water in nanometric cavities.[23−25] The

dx.doi.org/10.1021/jp307826s | J. Phys. Chem. C 2012, 116, 24340−24349

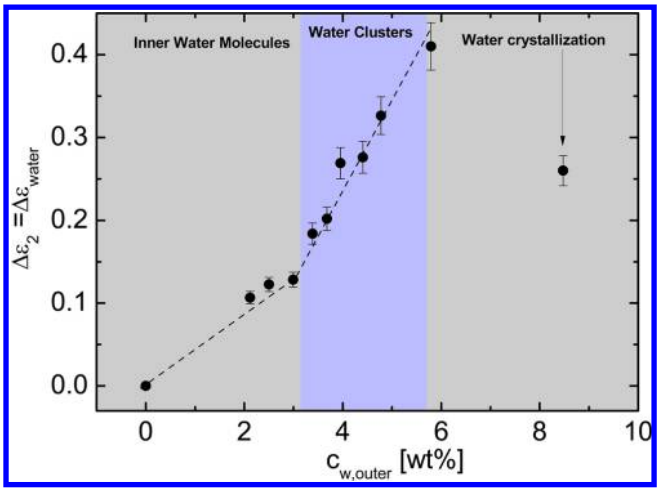

Figure 7. Relaxation strength ($\Delta\varepsilon_2$) as a function of water content for process 2. Error bars are indicated in the plot. "Inner water molecules" indicate water molecules in the internal surface of the silica particles (no rotational water). The label "Water clusters" refers to the ability of water molecules to join together instead of being uniformly distributed; "water crystallization" refers to the ability of water to crystallize at a high c_w, as seen by DSC.

assignment of this relaxation as due to the reorientation of the hydrated hydroxyl groups in the silanol groups is consistent with the small variation of the dielectric strength ($\Delta\varepsilon_3$) observed with increasing hydration (see next section) and similar with dry xerogel and dry MCM41.[13,16]

Finally, we also studied a sample dried at 373 K (S-373K). The total water content for this sample is 4.88 wt %. If we considered that the 2.76 wt % corresponds with the "inner water" then we can define a water content, $c_{w,outer} = c_{w,total} - 2.76$ wt %, which represents the fraction of water mainly located on the outer surface of the silica particles. Table 1 shows $c_{w,outer}$ for all of the samples analyzed in this work. For sample S-373K, a new relaxation process emerges (process 2). The strength of this process increases rapidly with water content (as we will see in the next section), and therefore, it is assigned to the reorientation of water molecules located at the outer surface of the silica particles. In addition, process 3 is still visible at lower frequencies, and its intensity is 3 times higher than that of sample S-393K. When annealing at 373 K (instead of 393K), a more hydroxylated surface is obtained, and it is likely that the intensity of process 3 increases. In addition, as more water molecules are present in the samples, its relaxation strength also increases.

The relaxation time corresponding to process 3 for S-373K is slower than that of S-393K. This is likely because water molecules bonded to hydroxyl groups prevent its reorientation, and therefore the relaxation becomes slightly slower. In addition, the activation energy is 0.62 eV. This energy value is similar to that found in reference 26, studying adsorption of water on silica surfaces. In that case, the heat of adsorption was found in the interval from 0.62 to 0.93 eV, and it was associated with the strong interaction of molecular water on pairs of interacting silanols in agreement with our interpretation. Figure 9 (panels a and b) shows a schematic drawing of our model for dried silica nanoparticles as deduced from the analysis of the dielectric response.

Dielectric Response of Hydrated Silica Particles. Now we focus the attention on the hydrated silica particles. Figure 6b shows the rapid increment of process 2 by adding water. This

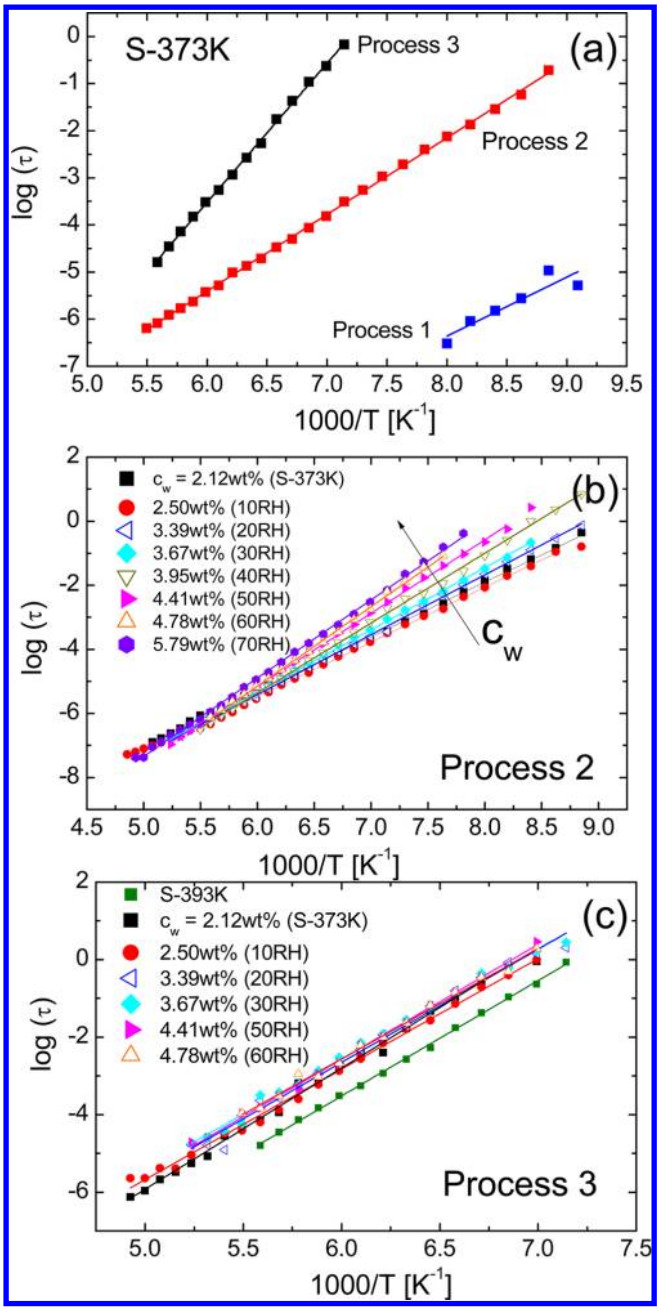

Figure 8. Plot of the characteristic relaxation times (τ) for all of the samples analyzed in this work. (a) Temperature dependence of τ for sample S-373K. The three relaxation processes (1, 2, and 3) can be observed. (b) Temperature dependence of τ corresponding to process 2 with a different water content. The relaxation time becomes slower by increasing the water content. (c) Temperature dependence of τ corresponding to process 3 with a different water content. The solid lines are fits of the Arrhenius equation to the data.

fact leads to infer that this relaxation is related with the reorientation of water molecules. In fact, this process has already been observed in a variety of water containing systems by several different experimental techniques[12,13,16,25−31] and also in hydrated silica-filled rubbers.[19] Figure 7 shows the variation of the average relaxation strength ($\Delta\varepsilon_2$) with the water content. $\Delta\varepsilon_2$ increases moderately with increasing concentration until $c_{w,outer}$ = 2.5 wt %. After that, a much stronger increment is observed which indicates a larger dipole moment reorientation in the high water concentration range.

dx.doi.org/10.1021/jp307826s | J. Phys. Chem. C 2012, 116, 24340−24349

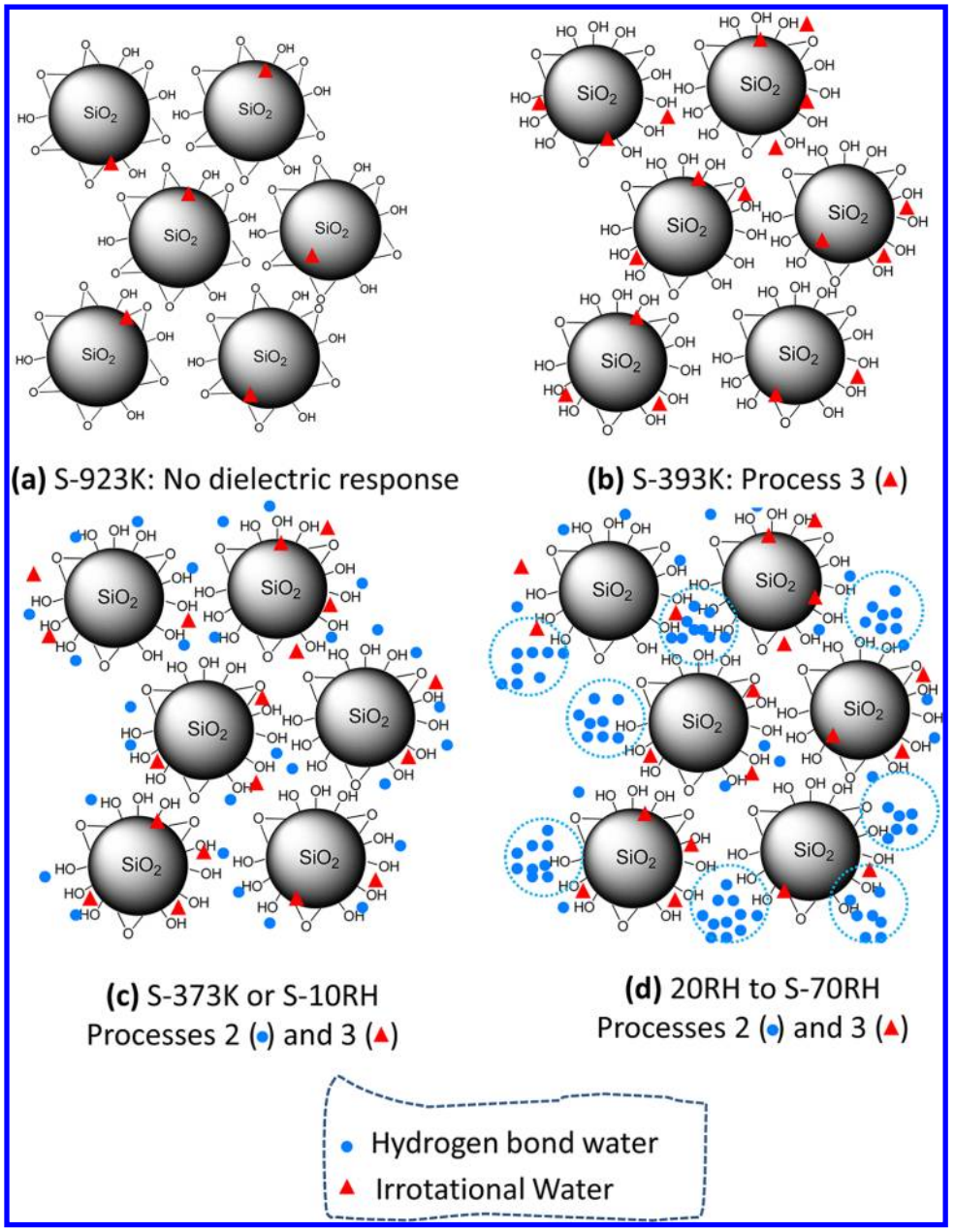

Figure 9. Schematic drawing of the water adsorbed at the surface of the silica particle at different hydration levels. (a) For S-923K only siloxanes, free silanols, and a few water molecules (which are bound in the inner surface) are present. No dielectric processes are observed, and therefore all of these groups (irrotational water and siloxanes) do not contribute to the dielectric response. (b) For S-393K, silanol groups are present at the surface of silica particles as well as water molecules. These water molecules cannot lead to a dielectric process and therefore are still irrotational. Process 3 appears in the dielectric response originating from the hydrated silanol groups. (c) S-373 and S-10RH: A new dielectric process appears in the dielectric spectra (process 2). At these low hydration levels, extra water molecules (located in the external surface of the silica particles) have more mobility than the previous ones. (d) S-20RH up to S70RH: Further water molecules prefer to join other water molecules (forming clusters) instead of distributing homogeneously. Circles indicate clustering of water.

Finally when water crystallizes, the dielectric signal falls because less water molecules are involved in the relaxation as some of them become part of the water crystals. The dependence of $\Delta\varepsilon_2$ with concentration is typically observed in other water solutions[29,30] and also in hard confinements.[22,23]

In addition, the temperature dependence of the relaxation times follows the Arrhenius behavior for all the water concentrations, characteristic of a local or secondary relaxation as pointed out by some of us[32] and by other authors.[12,31,33] The activation energy increases with water content from 0.34 eV for 2.12 wt % to 0.52 eV for 8.47 wt %. This last energy value is compatible with that associated with the dielectric reorientation of water molecules having a large mean number of hydrogen bonds (0.54 ± 0.4 eV).[25] At the same time, the value of τ_0 (obtained from the Arrhenius fit) is lower than 10^{-14} (the reciprocal of typical vibrational frequencies) for all c_w, until it reaches the unphysical value of $\log(\tau_o) = -20.66$ for sample S-80RH. Moreover, even for low water content, $\log(\tau_o)$ is less than 10^{-14}. This indicates that the local water relaxations do not fit Starkweather's definition[34,35] of a simple relaxation, showing cooperative effects. This suggests that water molecules do not distribute uniformly, but likely they go first to the more

dx.doi.org/10.1021/jp307826s | J. Phys. Chem. C 2012, 116, 24340−24349

favorable sites, as also suggested by the behavior of the relaxation strength (Figure 7). Consequently, our picture is consistent with the fact that water molecules prefer to form clusters from the initial stages of hydration instead of forming uniform layers of adsorbed water around the particles. This explanation is compatible with simulations of water in the amorphous silica surface[22], and that behavior was due to the presence of hydrophobic patches formed by siloxane groups. Figure 9 (panels c and d) shows a schematic drawing of our model for hydrated silica nanoparticles.

Now we focus on the temperature dependence of the water relaxation time corresponding with process 2. On the basis of previous results of water dynamics in mixtures of glasses and proteins (soft confinement)[25,31,36,37] or hard confinements,[12,16,23,24] the temperature dependence of the relaxation time of the water dynamics was found to show a crossover from low temperature Arrhenius behavior to another Arrhenius or Vogel−Fulcher−Tamman (VFT) behavior at higher temperatures. The origin of this crossover is still controversial in the literature, and it was related with (a) the existence of a fragile to strong transition related with that predicted for bulk water,[38] (b) the splitting of α- and β-relaxation,[39] and (c) as due to the intrinsic property of a Johari−Goldstein (JG) relaxation (water was identified as a JG relaxation),[40,41] or (d) the onset of finite size effects due to soft- or hard-confinement.[23,24,27]

For water around silica particles, we do not observe such crossover. Instead, the temperature dependence of the relaxation time is Arrhenius type on the whole temperature range analyzed. The absence of this crossover was also reported by Mamontov et al.[42] in studies of water on rutile (TiO_2 nanoparticles) from quasielastic neutron scattering (QENS) experiments for water content below one monolayer. However, a crossover was reported at higher hydration levels. Contrarily, water in silica particles retains the Arrhenius behavior even for high water content. For water confined in MCM-41 such crossover was observed at T ∼ 180 K[12] or at T ∼190 K.[16] Note that in both cases (MCM-41 and silica particles), the surface contains similar silanol groups. The main difference between these two systems is the fact that in MCM-41, water is confined in nanopores (∼10 Å), whereas in the surface of the silica particles this restriction does not emerge since water molecules are located on the external surface. Therefore, from our point of view, it is likely that the presence of a crossover in the temperature dependence of the relaxation time (around 160−200 K) is related with finite size effects, and it cannot be observed for water in silica particles because there is no spatial restriction for water molecules.

Finally, focusing on the slower process 3, we note that the activation energy does not show a large variation with increasing hydration having an average value of about 0.60 eV for the different water content. As this process was attributed to the dynamics of hydrated silanol groups and for all the hydrated samples, the number of reactive silanol groups per unit area should be the same, it is reasonable that both the activation energy and the relaxation strength do not increase with the water content.

CONCLUSIONS

We have systematically explored the effect of hydration on the dielectric properties of silica nanoparticles. On the basis of our results, two relaxation processes are evident, and they were related with hydrated silanol groups (process 3) and hydration water (process 2). By increasing the degree of hydration, it is possible to observe that water molecules prefer to form clusters. The results also show that the water relaxation depends on water content, whereas the relaxation corresponding to hydrated silanol groups is almost independent of the hydration level. Contrary to the observed behavior of water molecules in hard confinement, the temperature dependence of the relaxation time corresponding to process 2 is Arrhenius-like in the whole concentration and temperature range (i.e., the relaxation time does not exhibit any fragile-to-strong transition).

ASSOCIATED CONTENT

Supporting Information

Figure S1 shows the temperature dependence of the relaxation strength, and Figure S2 shows the temperature dependence of the broadening parameter. This material is available free of charge via the Internet at http://pubs.acs.org.

AUTHOR INFORMATION

Corresponding Author

*E-mail: scerveny@ehu.es.

Notes

The authors declare no competing financial interest.

ACKNOWLEDGMENTS

The authors gratefully acknowledge the support of the Spanish Ministry of Education

(MAT2007-63681), the Basque Government (IT-436-07), and the nano-IKER project. The continuous outstanding collaboration and support by Dr. F. Petry and Dr. R. Mruk (Goodyear Innovation Center Luxembourg) is also greatly acknowledged. We also thank the Goodyear Tire and Rubber Company for the permission to publish this paper.

REFERENCES

(1) *Colloidal Silica: Fundamentals and Applications*; Bergna, H. E., Roberts, W. O., Eds.; CRC Press: Boca Raton, FL, 2006.

(2) Flörke, O. W.; Graetsch, H. A.; Brunk, F.; Benda, L.; Paschen, S.; Bergna, H. E.; Roberts, W. O.; Welsh, W. A.; Libanati, C.; Ettlinger, M.; Kerner, D.; Maier, M.; Meon, W.; Schmoll, R.; Gies, H.; Schiffmann, D.Silica. In *Ullmann's Encyclopedia of Industrial Chemistry*; Wiley-VCH: New York, 2008.

(3) Young, G. J. *J. Colloid Sci.* **1958**, *13*, 67.

(4) (a) Klüppel M.; Fritzsche J. Constitutive Models for Rubber VI; Heinrich, G., Kaliske, M., Lion, A., et al., Eds.; 2010; p. 111. (b) Leblanc, J. L. *Prog. Polym. Sci.* **2002**, *27*, 627−687. (c) Klüppel, M. *Adv. Polym. Sci.* **2003**, *164*, 1−86.

(5) Ek, S.; Root, A.; Peussa, M.; Niinisto, L. *Themochimica Acta* **2001**, *379*, 201−212.

(6) Dimitrijevic, N. M.; Henglein, A.; Meisel, D. *J. Phys. Chem. B* **1999**, *103*, 7073−7076.

(7) Zhao, X. S.; Lu, G. Q.; Whittaker, A. K.; Millar, G. J.; Zhu, H. Y. *J. Phys. Chem. B* **1997**, *101*, 6525−6531.

(8) Kim, J. M.; Chang, S. M.; Kong, S. M.; Kim, K. S.; Kim, J.; Kim, W. S. *Ceram. Int.* **2009**, *35*, 1015−1019.

(9) de Farias, R. F.; Airoldi, C. *J. Therm. Anal. Calorim.* **1998**, *53*, 751−756.

(10) Yalamanchili, M. R.; Atia, A. A.; Miller, J. D. *Langmuir* **1996**, *12*, 4176−4184.

(11) Dijkstra, T. W.; Duchateau, R; van Santen, R. A.; Meetsma, A.; Yap, G. P. A. *J. Am. Chem. Soc.* **2002**, *124*, 9856−9864.

(12) Sjostrom, J.; Swenson, J.; Bergman, R.; Kittaka, S. *J. Chem. Phys.* **2008**, *128*, 154503.

(13) Spanoudaki, A.; Albela, B.; Bonneviot, L.; Peyrard, M. *Eur. Phys. J. E: Soft Matter Biol. Phys.* **2007**, *17*, 21.

(14) Jansson, H.; Swenson, J. *Eur. Phys. J. E: Soft Matter Biol. Phys.* **2003**, *12*, S51.
(15) Frunza, L.; Kosslick, H.; Pitsch, I.; Frunza, S.; Schönhals, A. *J. Phys. Chem. B* **2005**, *109*, 9154.
(16) Bruni, F.; Mancinelli, R.; Ricci, M. A. *Phys. Chem. Chem. Phys.* **2011**, *13*, 19773−19779.
(17) Zhuravlev, L. T. *Colloids Surf., A* **2000**, *173*, 1.
(18) Zhuravlev, L. T. *Langmuir* **1987**, *3*, 316−318.
(19) Meier, J. G.; Fritzsche, J.; Guy, L.; Bomal, Y.; Klüppel, M. *Macromolecules* **2009**, *42*, 2127.
(20) Kremer, F.; Schönhals, A. *Broadband Dielectric Spectroscopy*; Springer: Berlin, 2003.
(21) Cole, R. H.; Cole, K. S. *J. Chem. Phys.* **1942**, *10*, 98.
(22) Hassanali, A. A.; Singer, S. J. *J. Phys. Chem. B* **2007**, *111*, 11181.
(23) Cerveny, S.; Barroso-Bujans, F.; Alegría, A.; Colmenero, J. *J. Phys. Chem. C* **2010**, *114*, 2604.
(24) Cerveny, S.; Arrese-Igor, S.; Dolado, J. S.; Gaitero, J. J.; Alegría, A.; Colmenero, J. *J. Chem. Phys.* **2011**, *134*, 034509.
(25) Cerveny, S.; Colmenero, J; Alegria, A. *J. Non-Cryst. Solids* **2007**, *353*, 4523−4527.
(26) Dorémieux-Morin, C.; Heeribout, L.; Dumousseaux, C.; Fraissard, J.; Hommel, H.; Legrand, A. P. *J. Am. Chem. Soc.* **1996**, *118*, 13040.
(27) Cerveny, S.; Colmenero, J.; Alegria, A. *Phys. Rev. E: Stat. Phys., Plasmas, Fluids, Relat. Interdiscip. Top.* **2008**, *77*, 031803.
(28) Cerveny, S.; Alegria, A.; Colmenero, J. *The European Physical Journal Special Topics* **2007**, *141*, 49.
(29) (a) Pagnotta, S. E.; Cerveny, S.; Alegria, A.; Colmenero, J. *J. Chem. Phys.* **2009**, *131*, 085102. (b) Pagnotta, S. E.; Cerveny, S.; Alegria, A.; Colmenero, J. *Phys. Chem. Chem. Phys.* **2010**, *35*, 10512.
(30) Cerveny, S.; Alegria, A.; Colmenero, J. *J. Chem. Phys.* **2008**, *128*, 044901.
(31) Gainaru, C.; Schildmann, S.; Böhmer, R. *J. Phys. Chem. B* **2009**, *113*, 12628−12631.
(32) Cerveny, S.; Schwartz, G. A.; Bergman, R.; Swenson, J. *Phys. Rev. Lett.* **2004**, *93*, 245702.
(33) Capaccioli, S.; Ngai, K. L.; Shinyashiki, N. *J. Phys. Chem. B* **2007**, *111*, 8197−8209.
(34) Starkweather, H. W., Jr. *Macromolecules* **1981**, *14*, 1277−1281.
(35) Starkweather, H. W., Jr. *Polymer* **1991**, *32*, 2443−2448.
(36) Vogel, M. *Phys. Rev. Lett.* **2008**, *101*, 225701.
(37) Lusceac, S. A.; Gainaru, C.; Ratzke, D. A.; Graf, M. F.; Vogel, M. *J. Phys. Chem. B* **2011**, *115*, 11588.
(38) Chen, S. H.; Liu, L.; Fratini, E.; Baglioni, P.; Faraone, A.; Mamontov, E. *Proc. Natl. Acad. Sci. U.S.A.* **2006**, *103*, 9012−9016.
(39) Swenson, J.; Jansson, H.; Bergman, R. *Phys. Rev. Lett.* **2006**, *96*, 247802.
(40) Ngai, K. L.; Capaccioli, S. *J. Am. Ceram. Soc.* **2008**, *91*, 709.
(41) Capaccioli, S.; Ngai, K. L.; Ancherbak, S.; Rolla, P. A.; Shinyashiki, N. *J. Non-Cryst. Solids* **2011**, *357*, 641.
(42) Mamontov, E.; Vicek, L.; Wesolowski, D. J.; Cummings, P. T.; Rosenqvist, J.; Wang, W.; Cole, D. R.; Anovitz, L. M.; Gasparovic, G. *Phys. Rev. E: Stat. Phys., Plasmas, Fluids, Relat. Interdiscip. Top.* **2009**, *79*, 51504.

Macromolecules

Article

pubs.acs.org/Macromolecules

Influence of Water and Filler Content on the Dielectric Response of Silica-Filled Rubber Compounds

J. Otegui,[†] G. A. Schwartz,*[,†,‡] S. Cerveny,[†,‡] and J. Colmenero[†,‡,§]

[†]Centro de Física de Materiales (CSIC-UPV/EHU)-Material Physics Centre (MPC), P. M. de Lardizábal 5, 20018, San Sebastián, Spain

[‡]Donostia Internacional Physics Center, Paseo Manuel de Lardizábal 4, 20018, San Sebastián, Spain

[§]Departamento de Física de Materiales, Universidad del País Vasco (UPV/EHU), Facultad de Química, Apartado 1072, 20018, San Sebastián, Spain

J. Loichen and S. Westermann

Goodyear Innovation Center Luxembourg, Global Materials Science, Av. Gordon Smith, L-7750 Colmar-Berg, Luxembourg

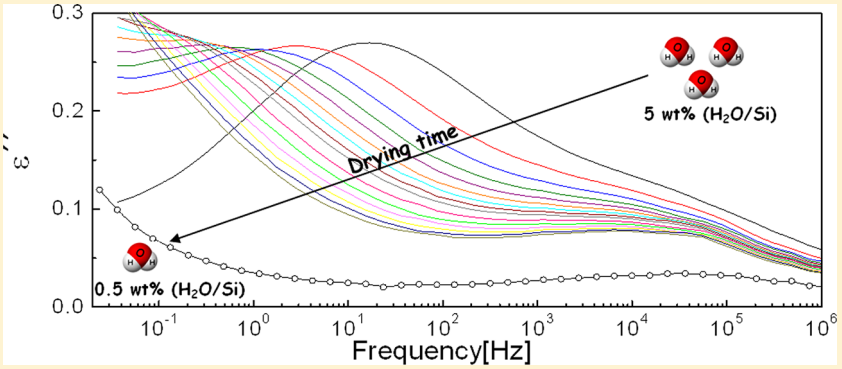

ABSTRACT: We present in this work a systematic study to analyze the influence of water and filler content on the dielectric response of silica-filled rubber compounds. For nanoparticle-filled polymers an additional dielectric process is usually observed in the loss dielectric spectra at frequencies lower than the alpha (α) or segmental relaxation. This process has generated some controversy in the literature due to the different (sometimes contradictory) interpretations given to explain its physical origin. We demonstrate, by means of dielectric spectroscopy in combination with thermal analysis, that this low-frequency process is compatible with a MWS process enhanced by the presence of water molecules at the silica surface. We show that the frequency of the maximum for this process is strongly affected by the amount of water attached to the silica particles. The dielectric response of the MWS process is rationalized by means of a simple interlayer model (IL). In addition, we also study the influence of water and filler content on the segmental dynamics and discuss possible mechanisms for the filler−polymer interaction.

1. INTRODUCTION

Reinforcement of polymers by nanoparticles plays an important role in improving the mechanical properties of polymeric compounds. In particular, styrene−butadiene rubber (SBR) filled with silica particles is widely used in numerous applications—the most important being the tire compounds.[1] This is because silica reduces the rolling resistance leading to lower fuel consumption and provides greater wear resistance and superior wet traction.[2,3] One of the key factors that determine the final properties of the filled compounds is the filler−polymer interaction, which strongly depends on several factors like polymer and filler type, filler surface treatment, chemical additives, and mixing procedure, among others. Several works have been published during the past years concerning the polymer dynamics of unfilled[4−7] and filled rubber compounds[8−11] and especially on the polymer−filler interaction.[12−15] However, despite the big effort done in this area, this interaction is far from being well understood, and contradictory interpretations can be found in the literature.

A powerful tool for investigating the polymer dynamics as well as the polymer−filler interaction in nanoparticles filled compounds is broadband dielectric spectroscopy (BDS).[16] This technique allows measuring the dielectric response over a broad frequency and temperature range, giving valuable information about both the molecular dynamics of the polymer chains and the polymer−filler interface. For unfilled SBR two relaxation processes are usually observed in the dielectric spectra:[7] the α-relaxation, involving cooperative motions, and the secondary

Received: November 21, 2012
Revised: February 11, 2013

   dx.doi.org/10.1021/ma302408z | *Macromolecules* XXXX, XXX, XXX−XXX

(or β-) relaxation, concerning the local motions (in polymers, the β-process can be usually related with the movement of lateral groups). However, when nanoparticles are added to SBR, an additional dielectric process is observed at frequencies lower than the α-relaxation. According to some authors, this process is caused by blocking of charge carriers at internal surfaces of different phases (interfaces) having different values of the dielectric permittivity and/or conductivity.[17,18] It is well-known that heterogeneous systems including interfaces (such as particle suspensions,[19,20] semicrystalline polymers,[21] blends,[22,23] and nanocomposite materials[24−28]) usually show a dielectric process attributed to the Maxwell−Wagner−Sillars (MWS) polarization. This process has been observed for rubber systems filled with carbon black,[29] graphite,[30] and silica.[11,31]

On the other hand, some researchers attribute this process to a second α-relaxation process associated with the polymer fraction attached to the filler particles.[32,33] For polymeric nanocomposites, a significant fraction of the polymer is within a distance of a few nanometers from the particle surface. According to these works, this interfacial polymer should have different structural and dynamics properties. It is argued that this thin layer of interfacial polymer has a restricted mobility due to the strong interaction between filler and polymer, being the origin of this second α-relaxation process.

The main purpose of this work is to establish that the origin of the low-frequency process observed for silica-filled SBR compounds in BDS is the MWS polarization. In addition, we will show that this process is enhanced by the presence of water molecules at the silica surface. The experimental data are well described by a simple model, which considers the water layer around the silica particles dispersed in the SBR matrix. In addition, we will analyze how water molecules affect the dielectric properties of silica SBR nanocomposites by studying the effect of drying and rehydrating. Finally, we will also discuss how the filler and water content affects the α-relaxation process.

2. EXPERIMENTAL SECTION

2.1. Materials. The polymer used in this work was solution styrene−butadiene rubber (S-SBR) BUNA VSL 5025. S-SBR has 25% styrene, 50% 1−2 vinyl, 15.4% 1−4 trans, and 9.6% 1−4 cis comonomer distribution. The filler used was precipitated amorphous silica (Z1165 MP-Rhodia) with a specific surface area of 165.8 m^2/g. Compounds with three different volume fraction of filler (0, 30, and 90 phr, where phr = per hundred rubber (parts in weight per 100 parts of rubber)) were prepared (see Table 1 for the composition of each sample). An internal mixer was used for mixing the rubber, the filler, and the rest of the additives. Once the compounds were mixed, square sheets were obtained by compression-molding vulcanization at 170 °C for 10 min in a mold yielding samples of 15 × 15 cm and thickness of about 0.7 mm. The samples from this batch were called "as-received" (AR) samples. Finally, different drying protocols were applied to the AR samples as explained in the next sections.

Table 1. Composition for Unfilled and Filled Compounds

components	unfilled	30 phr[a]	90 phr[a]
rubber (BUNA VSL 5025_0)	100	100	100
silica filler (Rhodia Z1165MP)		30	90
TESPD (link agent) bis(3-triethoxysilylpropyl) disulfide		2.4	7.2
antioxidant [*N*-(1,3)-dimethylbutyl-*N*′-phenyl-*p*-phenylenediamine]	2.5	2.5	2.5
stearic acid	3	3	3
TDAE oil	15	15	15
zinc oxide	2.5	2.5	2.5
accelerator [*N*-cyclohexyl-2-benzothiazolesulfeneamide]	2.3	2.3	2.3
sulfur	1.5	1.5	1.5
DPG secondary accelerator, diphenylguanidine		1	2

[a]phr = per hundred rubber.

2.2. Vacuum Drying (VD). The "as-received" (AR) samples were dried at 100 °C in a vacuum oven for 3 days. At this temperature most of the water was evaporated.

2.3. Rehydration Process (R). After vacuum drying, the samples were transferred to a hydration chamber where both the relative humidity (RH) and the temperature can be controlled. Rubber compounds were rehydrated by exposing them to different relative humidity levels (from 10RH to 70RH) at a temperature of 22 °C. The samples were maintained at constant relative humidity for 4 days in order to achieve the equilibrium for each hydration level. Once the samples were rehydrated to the desired level, they were immediately measured by BDS and TGA.

2.4. BDS Drying (BDSD). The samples were also dried inside the BDS cryostat (under a nitrogen atmosphere) according to the following procedure: first, we measured the dielectric signal at 295 K in the frequency range from 10^{-2} to 10^6 Hz. After that, the sample was dried by heating it at 100 °C for 40 or 90 min depending on the filler content. The dielectric spectrum was then measured again at 295 K, completing one measurement cycle. This procedure was repeated for 800 and 2130 min for 30 and 90 phr, respectively. At the end of the dielectric measurement, TGA were carried out to obtain the corresponding water content.

2.5. Differential Scanning Calorimetry (DSC). DSC measurements were performed by using a DSC Q2000 from TA Instruments in the standard mode. A cooling−heating cycle between −125 and 50 °C with a rate of 10 °C/min was performed using nitrogen as transfer gas. The annealing time between cooling and heating runs was 5 min. Hermetic aluminum pans were used. The glass transition temperature (T_g) was determined at the inflection point of the endotherm curve.

2.6. Thermogravimetry Analysis (TGA). Thermogravimetry measurements were performed for the three "as-received" SBR compounds (unfilled, 30 phr, and 90 phr) focusing on the water evaporation. The measurements were performed using a TGA-Q500 (TA Instruments). All the measurements were conducted under high-purity nitrogen flow over the temperature range 30−1000 °C with a ramp rate of 5 °C/min. In TGA experiments, the sample weight loss was recorded while the temperature was increased. The weight loss and its derivative with respect to the temperature give us valuable information about decomposition of the different components of the sample. In particular, this method is appropriate to determine the amount of water in the compounds.

2.7. TGA Method Used To Obtain the Water Content. Figure 1 shows typical thermographs for unfilled (a) and silica filled SBR compounds (b). In these curves, up to three different weight drops (or three peaks in the derivative plot) are observed. In the case of unfilled SBR (see Figure 1a) two peaks are visible; one around 200 °C (associated with oil evaporation[34]) and the other one between 300 and 450 °C (due to rubber decomposition[34]). For filled compounds (see Figure 1b), an extra weight loss can be observed at low temperatures. The first rapid initial drop of the mass (from room temperature up to ∼200 °C) corresponds to the loss of water adsorbed on the surface of silica.[35,36] In the weight derivative plot this mass drop is seen as a peak, herein namely "water peak". Defining T_1 as the onset of the oil peak in the weight derivative plot (where most of the water has been evaporated) and using the weight percentage $m(T_1)$, we can obtain an estimation of the water content (c_w) in our compounds. This percentage is about 2 wt % for AR90phr and about 1 wt % for AR30phr (see Table 2). The water content normalized to the silica content in the compounds ($c_w/c_{Si} \times 100$) can be calculated dividing the total water content by the silica content after subtracting the final weight obtained for the unfilled SBR ($m_{1000\ °C}$) related with the nonvolatile components (ZnO) (see last column in Tables 2−4).

2.8. Broadband Dielectric Spectroscopy (BDS). Broadband dielectric spectroscopy (BDS) was performed on disk-shaped samples

dx.doi.org/10.1021/ma302408z | Macromolecules XXXX, XXX, XXX−XXX

$$\varepsilon_s = \varepsilon_m\left(\frac{1+2\phi_p}{1-\phi_p}\right) \quad (4)$$

$$\varepsilon_\infty = \varepsilon_m\frac{(\varepsilon_p+2\varepsilon_m)+2(\varepsilon_p-\varepsilon_m)\phi_p}{(\varepsilon_p+2\varepsilon_m)-(\varepsilon_p-\varepsilon_m)\phi_p} \quad (5)$$

$$\tau = \frac{\phi_p}{1-\phi_p}\frac{3\varepsilon_o}{2\sigma_l\phi_l}[(\varepsilon_p+2\varepsilon_m)-(\varepsilon_p-\varepsilon_m)\phi_p] \quad (6)$$

Our composites can be considered as a three-component system where the silica particles embedded in the SBR rubber matrix are surrounded by an interfacial layer of water. All the assumptions described above are fulfilled for our system, and therefore the IL model can be applied to predict the MWS process. However, our loss peak is much broader than a Debye-type peak. This is because in our compounds we have aggregates and agglomerates that give a distribution of size and distances among them. Thus, we replaced the Debye function in the IL model (which assumes well-dispersed spherical particles of the same size) by the Cole−Cole function in order to take into account the size distribution of the particles and aggregates.

The Cole−Cole shape parameter in eq 3 was taken from the experimental fitting of the corresponding loss spectra ($\alpha = 0.4$). The dielectric constant for the polymer matrix was determined from the low-frequency limit of the real part of the dielectric permittivity of the unfilled SBR sample ($\varepsilon_m = 3.4$). The dielectric permittivity of the silica particles ($\varepsilon_p = 1.8$) was taken from the literature.[52] The value of φ_l was calculated from the water content obtained by TGA considering the volume fraction in Table 1, and σ_l was left as a fitting parameter.

Figure 9 shows the experimental dielectric loss spectra for different samples, after subtracting the α-relaxation and conductivity contributions. In the same figure we show the description (solid lines) obtained by the IL model using the parameters as described in the previous paragraph and leaving σ_l as the only fitting parameter. We can observe an excellent agreement for the position of the dielectric loss peaks at different hydration levels. The inset in Figure 9 shows the so-obtained values for the conductivity of the water layer (σ_l) as a function of water content. We observe that σ_l has an exponential dependence with water content according to previous findings in other systems.[51] Concerning to the intensity of the dielectric response, the model does not precisely account for the dielectric strength observed in the experimental data. Slightly higher values are observed for the experimental dielectric response compared to those predicted by the IL model. We have to take into account that this model assumes spherical particles with homogeneous surface. However, it is well-known that silica particles have a porous and irregular surface[40] that gives more available silica surface (compared to spherical particles), and therefore a larger interlayer area is present in these compounds. The presence of the aggregates and their distribution could also have an influence on the intensity differences observed between the model and the experimental data. All these results allow us to conclude that the low-frequency process observed for these silica-filled SBR compounds is a MWS polarization process due to the different dielectric permittivity between filler and polymer, enhanced by the presence of water molecules around the silica particles.

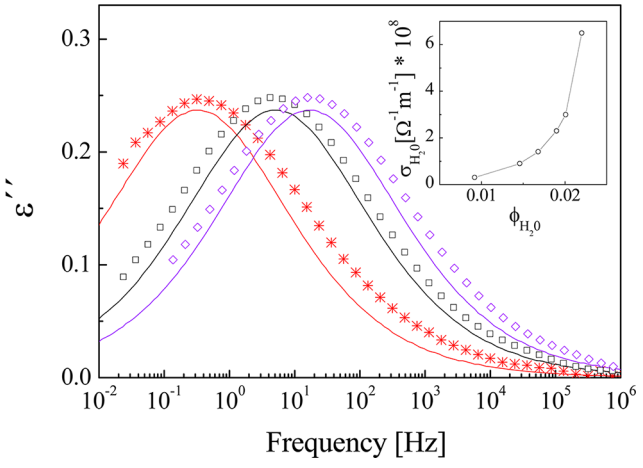

Figure 9. Dielectric loss spectra at fixed temperature (295 K) for R30phr 10% RH (red ∗), AR30phr (black □), and R30phr 70% RH (purple ◇) samples, after subtracting the α-relaxation and conductivity contributions. Solid lines represent the interlayer model (IL) descriptions. Inset: interlayer conductivity σ_l as a function of water volume fraction φ_l.

4.2. Interfacial Polymer around Silica Particles. As already mentioned, it has been argued[32] that the process observed at frequencies lower than the α-relaxation is due to the reduced mobility of SBR at the interface, i.e., polymer segments which are adsorbed at the surface of the nanofillers. Moreover, an effective dielectric glass transition temperature associated with this slow dielectric process (more than 65 °C higher than the bulk glass transition temperature) has been reported.[32] In principle, two glass transitions should be observed by DSC as two separated steps or at least as a very broad single step. However, these features were not observed by us (see Figure 10). Instead, a single glass transition at about

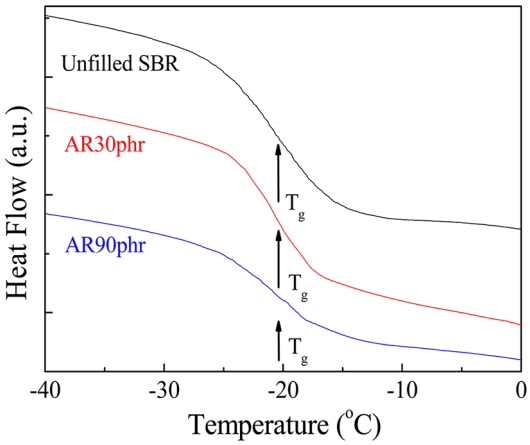

Figure 10. Heat flow as a function of the temperature as obtained from standard calorimetric measurements for unfilled SBR, AR30phr, and AR90phr samples.

252 K is seen for unfilled ($T_g = 252.6 \pm 0.2$ K) and AR silica filled SBR ($T_g = 252.4 \pm 0.3$ K for 30 phr and $T_g = 252.4 \pm 0.4$ K for 90 phr). It is also interesting to note that in these samples the silica nanoparticles do not affect the calorimetric glass transition temperature within the experimental error.

dx.doi.org/10.1021/ma302408z | Macromolecules XXXX, XXX, XXX−XXX

The process observed by Vo et al.[32] is similar to the low-frequency process observed by us in this work. However, we demonstrate in the previous section that this process is a MWS polarization enhanced by water molecules around silica particles. This fact does not mean there are no polymer chains interacting with the filler surface. However, from our results it is clear that the low-frequency process is not reflecting such behavior.

4.3. α-Relaxation. We will now turn to the effect of both water and filler content on the segmental dynamics of the SBR compounds. Following Figure 8, we can observe that the relaxation time is almost independent of water content and slightly depends (for 90 phr) on filler content. It has been observed for some aqueous polymeric solution that water acts as plasticizer increasing the mobility of the polymer and therefore decreasing the glass transition temperature. However, for the compounds here studied, we do not observe any shift in the calorimetric T_g or in the relaxation time. Thus, the segmental relaxation is almost unaffected by the water molecules. From this observation we can assume that, despite of the fact that the structure of our composite is rather complex, the absorbed water is only present at the filler−matrix interface, and therefore no plasticization of the matrix is produced. The absence of water molecules in the polymer matrix is also supported by the TGA measurements that show no water peak for unfilled samples.

The segmental dynamics of the polymeric matrix seems to be slightly (or even not) affected by the presence of the filler, in agreement with previous observations reported for SBR silica nanoparticle compounds[50] and also for other composites.[51−54] At 30 phr the difference is negligible, whereas for 90 phr a small difference is observed between unfilled and filled compounds. However, the dielectric T_g ($T_{g,100s}$) is not affected, and it is the same for all the compounds within the experimental error.

4.4. Polymer−Filler Interaction. Finally, we will focus on the polymer−filler interactions which in a coarse scheme can be divided into two groups: (1) chain segments directly bonded to the filler surface (e.g., chemisorbed) and (2) polymer−filler interaction mediated by coupling agents (e.g., bis(3-triethoxysilylpropyl) disulfide). The samples analyzed here correspond to the second case, where the coupling agent links filler particles to polymer chains through sulfur covalent bounds. This provides a relative flexible link between the polymer chains and the particles surface, and the overall effect is a slight increment of the effective cross-link density. This kind of interaction only slightly affects the α-relaxation of the polymer. In the case of chain segments directly bonded to the filler, the individual monomers are certainly immobilized at the surface, and therefore this kind of link is less flexible than the previous one. However, according to Robertson and Roland,[15] a large fraction of directly bonded segments are necessary to obtain an immobilized phase. This is because the segmental dynamics underlying the glass transition involves conformational transitions of only a few polymeric units. According to the Adam−Gibbs framework,[54] a cooperative rearrangement region (CRR) can be defined with a size related with the relevant length scale where the α-relaxation takes place. The size of the CRR has not been determined for SBR, but on the basis of measurements performed on similar polymers by means of mechanical,[52,53] dielectric,[54,55] and calorimetric methods,[56,57] we can estimate its value between 1 and 2 nm. This means that whatever is the kind of the polymer−filler interaction, it should not affect the segmental dynamics beyond 1 or 2 nm away from the link. Therefore, although there are some published works that seem to unambiguously show the presence of immobilized polymer segments at the surface of the filler particles, it is still not clear whether this polymer−filler interaction will significantly affect the segmental dynamics. We are currently running some experiments to study in depth the α-relaxation of the polymer close and far from the silica surface. These results will be published in a future work.

5. CONCLUSIONS

In this work we have studied the dielectric response of silica-filled SBR compounds. Two processes were observed in the dielectric spectra for the temperature and frequency range here analyzed. The faster process is associated with the segmental relaxation, whereas the slower one is related to the MWS polarization. It was found that the MWS process is directly related with the water layer around the silica particles. The amount of hydration water determines the position of the maximum in the loss spectrum. For high water contents, the MWS peak moves to higher frequencies, whereas for low water contents the peak shifts to lower frequencies. The MWS process can be completely removed from our experimental frequency window for extremely low water contents. This behavior has been rationalized by means of the IL model. With regards to the α-relaxation it was found that the position of the calorimetric glass transition is not affected by the addition of the filler or by the water content. Finally, we have also discussed possible mechanisms for the filler−polymer interaction and its influence on the polymer dynamics.

AUTHOR INFORMATION

Corresponding Author

*E-mail: schwartz@ehu.es.

Notes

The authors declare no competing financial interest.

ACKNOWLEDGMENTS

The authors gratefully acknowledge the support of the Spanish Ministry of Education (MAT2012-31088) and the Basque Government (IT-436-07). The continuous outstanding collaboration and support by Dr. F. Petry and Dr. R. Mruk (Goodyear Innovation Center Luxembourg) are also greatly acknowledged. We also thank the Goodyear Tire and Rubber Company for the permission to publish this paper.

REFERENCES

(1) Bergna, H. E.; Roberts, W. O. *Colloidal Silica: Fundamental and Applications*; CRC Press: Boca Raton, FL, 2006.
(2) Wolff, S.; Wang, M. J. *Rubber Chem. Technol.* **1992**, *65*, 329.
(3) Wang, M. J.; Wolff, S.; Tan, E. H. *Rubber Chem. Technol.* **1993**, *66*, 178.
(4) Klüppel, M.; Heinrich, G. *Macromolecules* **1994**, *27*, 3596.
(5) Klüppel, M. *Macromolecules* **1994**, *27*, 7179.
(6) Marzocca, A. J.; Cerveny, S.; Mendez, J. M. *Polym. Int.* **2000**, *49*, 216. Cerveny, S.; Ghilarducci, A.; Salva, H.; Marzocca, A. J. *Polymer* **2000**, *41*, 2227.
(7) Cerveny, S.; Bergman, R.; Schwartz, G. A.; Jacobsson, P. *Macromolecules* **2002**, *35*, 4337. Janik, P.; Paluch, M.; Ziolo, J.; Sulkowski, W.; Nikiel, L. *Phys. Rev. E* **2001**, *64*, 042502.
(8) Heinrich, G.; Klüppel, M. *Adv. Polym. Sci.* **2002**, *160*, 1.
(9) Klüppel, M. *Adv. Polym. Sci.* **2003**, *164*, 1.
(10) Ward, A. A.; Bishai, A. M.; Hanna, F. F.; Yehia, A. A.; Stoll, B.; von Soden, W.; Herminghaus, S.; Mansour, A. A. *Kaut. Gummi Kuns.* **2006**, 654.

(11) Meier, J. G.; Fritzsche, J.; Guy, L.; Bomal, Y.; Klüppel, M. *Macromolecules* **2009**, *42*, 2127.
(12) Heinrich, G.; Klüppel, M.; Vilgis, T. A. *Curr. Opin. Solid State Mater. Sci.* **2002**, *6*, 195.
(13) Arrighi, V.; McEwen, I. J.; Qian, H.; Serrano Prieto, M. B. *Polymer* **2003**, *44*, 6259.
(14) Schwartz, G. A.; Cerveny, S.; Marzocca, A. J.; Gerspacher, M.; Nikiel, L. *Polymer* **2003**, *44*, 7229.
(15) Robertson, C. G.; Roland, C. M. *Rubber Chem. Technol.* **2008**, *81*, 506.
(16) Kremer, F.; Schönhals, A. *Broadband Dielectric Spectroscopy*; Springer-Verlag: Berlin, 2003.
(17) Schönhals, A.; Goering, H.; Costa, F. R.; Wagenknecht, U.; Heinrich, G. *Macromolecules* **2009**, *42*, 4165.
(18) Asami, K. *Prog. Polym. Sci.* **2002**, *27*, 1617.
(19) Davis, L. C. *J. Appl. Phys.* **1992**, *72*, 1334.
(20) Rica, R. A.; Jiménez, M. L.; Delgado, A. V. *Soft Matter* **2012**, *8*, 3596.
(21) Arous, M.; Ben Arnor, I.; Kallel, A.; Fakhfakh, Z.; Perrier, G. *J. Phys. Chem. Solids* **2007**, *68*, 1405.
(22) Feldman, Y.; Skodvin, T.; Sjoblom, J. Dielectric Properties of Emulsion and Related Colloidal Systems. *Encyclopedic Handbook of Emulsion Technology*: Marcel Dekker: New York, 2000.
(23) Pratt, G. T.; Smith, M. J. A. *Polymer* **1989**, *30*, 1113.
(24) Lee, Y. H.; Bur, A. J.; Roth, S. C.; Start, P. R. *Macromolecules* **2005**, *38*, 3828.
(25) Bohning, M.; Goering, H.; Fritz, A.; Brzezinka, K. W.; Turky, G.; Schönhals, A.; Schartel, B. *Macromolecules* **2005**, *38*, 2764.
(26) Chanmal, C. V.; Jog, J. P. *Express Polym. Lett.* **2008**, *2*, 294.
(27) Meier, J. G.; Mani, J. W.; Klüppel, M. *Phys. Rev. B* **2007**, *75*, 054202.
(28) Carsi, M.; Sanchis, M. J.; Diaz-Calleja, Riande, R. E.; Nugent, M. J. D. *Macromolecules* **2012**, *45*, 3571.
(29) Leyva, M. E.; Barra, G. M. O.; Moreira, A. C. F.; Soares, B. G.; Khastgir, D. *J. Polym. Sci., Part B* **2003**, *41*, 2983.
(30) Mansour, S. A.; Al-ghoury, M. E.; Shalaan, E.; El Eraki, M. H. I.; Abdel-Bary, E. M. *J. Appl. Polym. Sci.* **2011**, *122*, 1226.
(31) Eid, M. A. M.; El-Nashar, D. E. *Polym.-Plast. Technol. Eng.* **2006**, *45*, 675.
(32) Vo, L. T.; Anastasiadis, S. H.; Giannelis, E. P. *Macromolecules* **2011**, *44*, 6162.
(33) Castagna, A. M.; Wang, W.; Winey, K. I.; Runt, J. *Macromolecules* **2011**, *44*, 2791.
(34) Fernández-Berridi, M. J.; González, N.; Mugica, A.; Bernicot, C. *Thermochim. Acta* **2006**, *444*, 65.
(35) Cerveny, S.; Schwartz, G. A.; Otegui, J.; Colmenero, J.; Loichen, J.; Westermann, S. *J. Phys. Chem. C* **2012**, *116*, 24340.
(36) Zhuravlev, L. T. *Colloids Surf., A* **2000**, *173*, 1.
(37) Hanna, F. F.; Bishai, A. M.; Ward, A. A.; Stoll, B.; Göritz, D. *Kaut. Gummi Kuns.* **2004**, *57*, 288.
(38) Nikaj, E.; Stevenson-Royaud, I.; Seytre, G.; David, L.; Espuche, E. *J. Non-Cryst. Solids* **2010**, *356*, 589.
(39) Cole, K. S.; Cole, R. H. *J. Chem. Phys.* **1941**, *9*, 341.
(40) (a) Vogel, H. *Phys. Z.* **1921**, *22*, 645. (b) Fulcher, G. S. *J. Am. Chem. Soc.* **1925**, *8*, 339. Fulcher, G. S. *J. Am. Chem. Soc.* **1925**, *8*, 789.
(41) Banhegyi, G.; Karasz, F. E. *J. Polym. Sci.* **1986**, *24*, 209.
(42) Woo, M.; Piggott, R. *J. Compos.* **1988**, *10*, 16.
(43) Van Beek, L. K. H. *Dielectric Behavior of Heterogeneous Systems*; Progress in Dielectrics Vol. *7*; Heywood Books: London, 1967.
(44) Banhegyi, G. *Colloid Polym. Sci.* **1986**, *264*, 1030.
(45) Dyre, J. C. *J. Phys. C* **1986**, *19*, 5655.
(46) Steeman, P. A. M.; Maurer, F. H. J. *Colloid Polym. Sci.* **1990**, *268*, 315.
(47) Pelster, R. *Phys. Rev. B* **1999**, *59*, 9214.
(48) Steeman, P. A. M.; Maurer, F. H. J.; van ES, M. A. *Polymer* **1991**, *32*, 523.
(49) Datta, S.; Bhattcharya, A. K.; De, S. K.; Kontos, E. G.; Wefer, J. M. *Polymer* **1996**, *37*, 5597.
(50) Fritzsche, J.; Klüppel, M.; Meier, J. G. *Kaut. Gummi Kuns.* **2009**, *62*, 319.
(51) Boucher, V. M.; Cangialosi, D.; Alegría, A.; Colmenero, J.; Gonzalez-Irun, J.; Liz-Marzan, L. M. *Soft Matter* **2010**, *6*, 3306.
(52) Boucher, V. M.; Cangialosi, D.; Alegría, A.; Colmenero, J.; Pastoriza-Santos, I.; Liz-Marzan, L. M. *Soft Matter* **2011**, *7*, 3607.
(53) Cangialosi, D.; Boucher, V. M.; Alegria, A.; Colmenero, J. *Polymer* **2012**, *53*, 1362.
(54) Bogoslovov, R. B.; Roland, C. M.; Ellis, A. R.; Randall, A. M.; Robertson, C. G. *Macromolecules* **2008**, *41*, 1289.
(55) Adam, G.; Gibbs, J. H. *J. Chem. Phys.* **1965**, *43*, 139.
(56) Povolo, F.; Hermida, E. B. *J. Appl. Polym. Sci.* **1995**, *58*, 55.
(57) Povolo, F.; Schwartz, G.; Hermida, E. B. *J. Polym. Sci., Part B: Polym. Phys.* **1996**, *34*, 1257.
(58) Schwartz, G. A.; Cangialosi, D.; Alegría, A.; Colmenero, J. *J. Chem. Phys.* **2006**, *124*, 154904.
(59) Cangialosi, D.; Alegría, A.; Colmenero, J. *Phys. Rev. E* **2007**, *76*, 011514.
(60) Donth, E. *J. Non-Cryst. Solids* **1982**, *53*, 325.
(61) Cerveny, S.; Mattsson, J.; Swenson, J.; Bergman, R. *J. Phys. Chem. B* **2004**, *108*, 11596.